# Compaction Bands in Porous Rock

J. W. Rudnicki
*Department of Mechanical Engineering, Northwestern University, Evanston, Illinois, USA*

In *Bifurcations and Instabilities in Geomechanics*, Proceedings of the International Workshop on Bifurcation and Instability 2002, St. John's College, Minnesota, June 3 –5, 2002, pp. 29 – 39. Editted by J. Labuz and A. Drescher. Swets & Zeitlinger (formerly Balkema) Publishers.

ABSTRACT: Compaction bands are localized, planar zones of compressed material that form perpendicular to the maximum compressive stress. Compaction bands have been observed in porous sandstone formations in the field and in laboratory compression tests on porous sandstone, plaster, glass beads, polycarbonate honeycombs and metal foams. Because the permeability of the compacted material is much reduced, compaction bands can form barriers to fluid flow and adversely affect attempts to inject or withdraw fluids from porous reservoirs. An analysis of conditions for the onset of compaction bands as a bifurcation from homogeneous deformation indicates that they can occur when the stress strain curve for uniaxial compressive deformation has a peak. Formation of compaction bands is favored by significant compactive inelastic deformation and by a reduction in the yield stress for shear with increasing compressive mean stress. These conditions are typical for stress states on a "cap" yield surface often used to model the inelastic deformation of porous geomaterials.

## 1 INTRODUCTION

Localized deformation in rocks and other geomaterials has been primarily associated with shear deformation. But Vardoulakis and Sulem (1995, p. 177) note that "compaction layering is observed in geomaterials at many scales." Furthermore, recent field and experimental observations in porous sandstones have identified localized, planar bands of material that has been compacted, without evident shear, relative to the adjacent material. The material in the band is less permeable than the surrounding material (Papamichos et al. 1993) and a decrease of an order of magnitude in permeability has been measured in recent experiments (Holcomb & Olsson, 2002).

Porous rock formations are exploited for a variety of human activities, e.g. recovery and storage of oil and gas, storage of water, disposal of hazardous waste products and sequestration of carbon dioxide to mitigate adverse effects on the atmosphere (Wawersik et al. 2001). Formation of compaction bands caused by stress changes due to the injection or withdrawal of fluid could dramatically alter the fluid flow properties of the formation and prevent efficient, safe and economic use. Compaction band formation is one possible explanation for localized compaction observed in producing oil fields (Nagel, 2001). Furthermore, because compaction bands are localized features, they will be difficult to detect by surface or borehole geophysical methods. Consequently, understanding the conditions that affect the formation and evolution of compaction bands is of practical importance.

Although this paper focuses on compaction bands in geomaterials, similar structures have been observed in a variety of other porous materials, including metal foams (Bastawros et al. 2000, Park & Nutt, 2001), polycarbonate honeycomb (Papka & Kyriakides, 1998), and snow (J. Desrues, pers. comm.). Formation of zones of localized deformation, either compaction or shear, can adversely affect forming processes of metal powders (Gu et al. 2001). Non-uniform density distributions resulting from cold compaction can result in shape distortions during sintering, and

final products with undesirable non-uniform properties. Although the micromechanical mechanisms of deformation are different in these various materials, similar phenomenological constitutive relations can be used to describe them (Gu et al. 2001). Thus, understanding the conditions for the occurrence of compaction bands is relevant to a variety of materials and technological processes.

This paper describes in more detail the nature of compaction bands in geomaterials, recent observations of them in laboratory experiments and analyses for their formation. The paper concludes with a discussion of open questions.

## 2 WHAT ARE COMPACTION BANDS?

Figure 1 shows schematically the formation of a shear band or fault in an axisymmetric compression experiment: relatively homogenous deformation (Fig. 1a) gives way to localized deformation in a narrow planar zone (Fig. 1b). Deformation in the zone is a combination of shear and dilation or compression relative to the plane of the band. The orientation of the band varies with rock type and the confining (lateral) stress but typically makes an angle of about $30^o$ with the direction of the axial compressive stress.

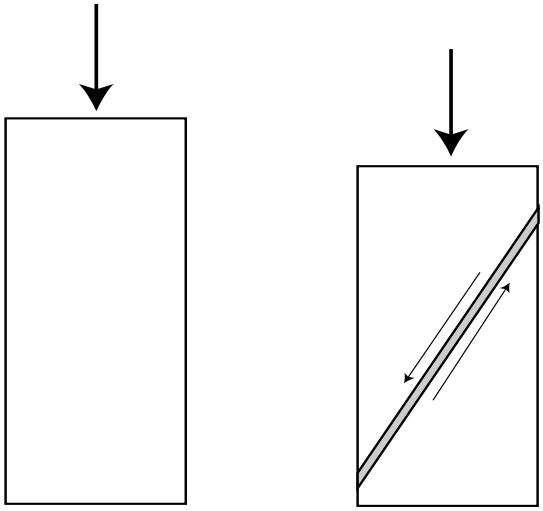


Figure 1. Schematic illustration of the formation of a shear band (b) following homogeneous deformation (a) in the axisymmetric compression test.

Figure 2 shows schematically the formation of a compaction band. In Figure 2b, axial compression occurs uniformly (the distance between the horizontal lines in Figure 2a is decreased uniformly in Figure 2b). In Figure 2c, compression occurs predominantly in a narrow zone, i.e. a compaction band; outside this zone much less compression occurs. The plane of the compaction band is perpendicular to the largest compressive principal stress.

Antonellini & Aydin (1995) and Mollema & Antonellini (1996) have reported observations of compaction bands in porous sandstone formations. Olsson (1999) identified examples of compaction bands in earlier laboratory experiments and reported observations of compaction bands in axisymmetric deformation experiments on Castlegate sandstone. Some of Olsson's samples contained both compaction and shear bands. Other recent observations of compaction bands in experiments have been reported by Olsson & Holcomb (2000), DiGiovanni et al. (2000), Olsson (2001), Olsson et al. (2002), Haimson (2001), Klein et al. (2001) and Wong et al. (2001).

The appearance of the compaction bands is, however, much different in the experiments of different groups. Olsson & Holcomb (2000), Olsson (2001) and Olsson et al. (2002) have used acoustic emissions and permeability measurements to infer a widening zone of compaction (Fig. 3a). The zone begins near the ends of the specimen and spreads behind a planar front that propagates with a speed roughly an order of magnitude greater than the piston velocity. Accord-

ing to the analysis of Olsson (2001), the speed of the propagating front is proportional to the porosity difference between the compacted and uncompacted portions of the specimen. In contrast, Klein et al. (2001) and Wong et al. (2001) observe thin planar zones of compacted material alternating with uncompacted material (Fig. 3b). These zones also begin near the specimen ends; increasing piston displacement causes progressive formation of additional zones farther from the ends. The sandstones tested by the two groups are different and it is unclear whether this or some other aspect of the testing is causing the different appearances of the compaction zones.

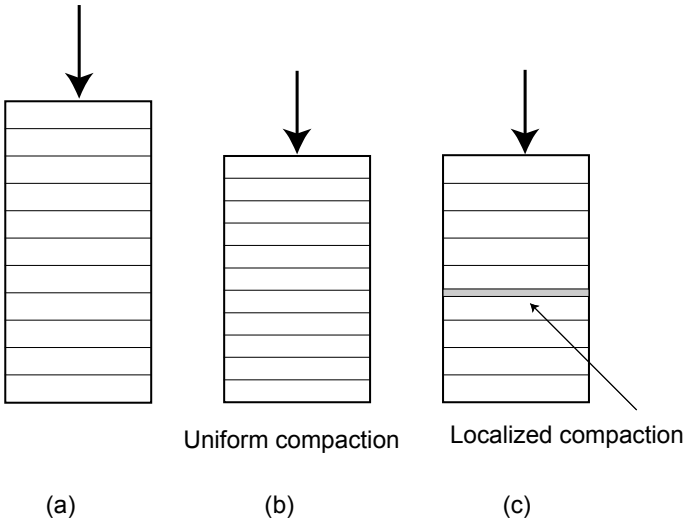


Figure 2. Schematic illustration of compaction band formation in the axisymmetric compression test. (a) undeformed specimen; (b) uniform compaction; (c) localized compaction band formation.

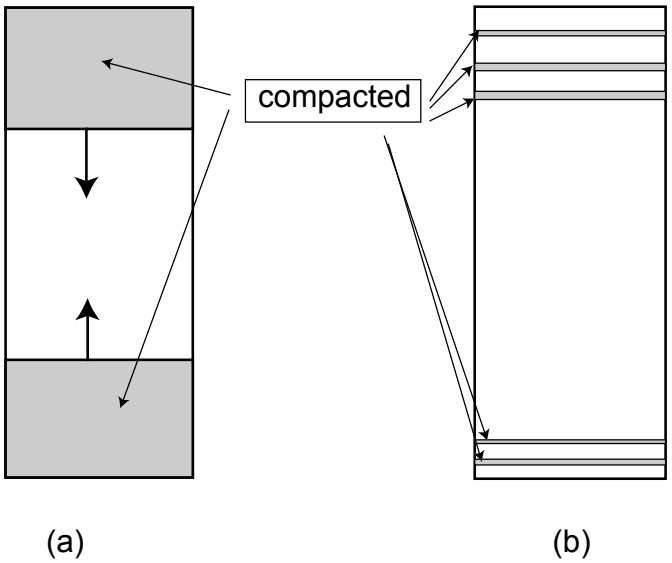


Figure 3. Different appearance of evolving compaction zones. In (a) the compacted zone widens and spreads across the specimen with increasing piston displacement; in (b) localized bands of compaction alternate with less compacted material; additional bands form farther from the ends as the piston displacement continues.

## 3 WHY DO COMPACTION BANDS FORM?

Olsson (1999) recognized that the inception of compaction bands could be addressed as a bifurcation from homogeneous deformation, the same approach used to study the inception of shear bands (Rudnicki & Rice, 1975, Rice, 1976). For boundary conditions that permit homogeneous deformation as a possible solution for the next increment of deformation, this approach seeks

conditions for which the formation of a band of localized deformation is an alternative solution. The formation of the band solutions is subject to conditions of compatibility and equilibrium.

The compatibility condition requires that velocities, or increments of displacement, are continuous at the instant of band formation. Consequently, the displacement increment within the band $du_i^{\text{band}}$ is related to the increment in the homogeneous field outside the band $du_i^0$ by

$$du_i^{\text{band}} = du_i^0 + \mathrm{g}_i(\mathbf{n}\bullet\mathbf{x}) \tag{1}$$

where $\mathbf{n}$ is the unit normal to the plane of the band and the $g_i$ are functions only of distance across the band. The corresponding strain increments are related by

$$d\varepsilon_{ij}^{\text{band}} = d\varepsilon_{ij}^0 + \frac{1}{2}(n_i g_j + g_i n_j) \tag{2}$$

For a compaction band the vector $\mathbf{g}$ is in the same direction as the normal but opposite in sense, $\mathbf{g} \propto -\mathbf{n}$. Thus, the difference in strain increments (2) is uniaxial.

Equilibrium requires that the increments of traction be continuous across the band interface at the onset of localization:

$$dt_i = n_j(d\sigma_{ji})^{\text{band}} = n_j(d\sigma_{ji})^0 \tag{3}$$

If the constitutive relation can be expressed in the incrementally linear form

$$d\sigma_{ij} = L_{ijkl}d\varepsilon_{kl} \tag{4}$$

then substituting (4) into (3) and using (2) yields the condition for localization:

$$n_i L_{ijkl} n_l g_k = 0 \tag{5}$$

In obtaining (5) it has been assumed, without loss of generality, that $L_{ijkl}$ is symmetric with respect to interchange of the first two and last two indices, but not necessarily with respect to interchange of the first and last pair. The result (5) also assumes that the response at the onset of band formation is the same both inside and outside of the band but Rice & Rudnicki (1980) have shown that for a wide class of material models this bifurcation precedes one that occurs with elastic unloading outside the band (Chambon (1986) has given a more general derivation of this result). Rice (1976) has given a more general formulation of the localization problem.

A non-zero solution for the $g_k$ (5), which expresses a nonuniform deformation field, is possible only if the determinant of the coefficient matrix vanishes. In general, the direction of $\mathbf{g}$ depends on the constitutive properties (Bésuelle, 2001), but for a compaction (or dilation) band, it is in the same direction as $\mathbf{n}$, i.e $\mathbf{g} = \alpha\mathbf{n}$ where $\alpha$ is a scalar. Substituting into (5) and multiplying by $n_j$ reveals that the condition for inception of a compaction or dilation band is that the tangent modulus for uniaxial deformation relative to the plane of the band must vanish. Thus, for a compaction (or dilation) band (5) requires that

$$n_i n_j L_{ijkl} n_k n_l = 0 \tag{6}$$

Olsson (1999) arrived at the same condition using a one-dimensional analysis and the results of Issen & Rudnicki (2000, 2001), who use the constitutive relation employed by Rudnicki & Rice (1975), can be expressed in the same form.

## 4 CONSTITUTIVE MODELS

### *4.1 Axisymmetric Compression*

Whether the condition (6) or (5) can be met obviously depends strongly on the type of constitutive model, i.e. the form of the $L_{ijkl}$. To illustrate the dependence on constitutive parameters in a simple way, consider the relation used by Rudnicki (1977, 2002) for axisymmetric deformation. The standard axisymmetric compression test is shown schematically in Figure 4a. If, as in the

most common test, the lateral stresses are held constant, the axial and lateral strain increments can be expressed as

$$d\varepsilon_{\text{axial}} = d\sigma_{\text{axial}} / E,\ d\varepsilon_{\text{lat}} = -\nu d\varepsilon_{\text{axial}} \tag{7}$$

Thus, $E$ is the tangent modulus for constant lateral confining stress and $\nu$ plays a role similar to Poisson's ratio but is a nonelastic parameter and may vary with the deformation (Fig. 4b). Additional constitutive parameters can be defined by increasing the lateral stress and adjusting the axial stress so that the axial deformation is held fixed. Then the increments of lateral strain and axial stress are expressed as

$$d\varepsilon_{\text{lat}} = 2d\sigma_{\text{lat}} / 9K,\ d\sigma_{\text{axial}} = rd\sigma_{\text{lat}} \tag{8}$$

The ratios $r$ and $\nu$ are normally positive, but Figure 5 shows a simple, pin-jointed model structure for which $r$ and $\nu$ are negative. Although this might be a plausible microstructural model for a very porous, open-cell material, it would seem less appropriate for most rocks or soils. Nevertheless, it does make clear that negative $r$ and $\nu$ are possible. An expression for the tangent modulus for uniaxial strain (zero lateral strain) can be obtained by combining (7) and (8), $E_{\text{uniaxial}} = E + 9Kr\nu/2$. Setting this value equal to zero yields the critical value of the tangent modulus for compaction band formation in a test with constant lateral confining stress:

$$E_{\text{crit}} = -9\nu rK/2 \tag{9}$$

Figure 6 shows a schematic illustration of a typical stress strain curve for a very porous sandstone (at relatively high confining pressure). Compaction bands, if they occur, form on the flat shelf of the stress strain curve where $E \approx 0$. Because the modulus $K$ is presumably positive, (9) implies that either $r$ or $\nu$ is near zero at compaction band formation. Experimental evidence on this issue is mixed. Figure 6 of Olsson (1999) shows constant lateral deformation at the mid-height of an axisymmetric compression sample indicating $\nu \approx 0$ but Wong et al. (2001) report increasing lateral deformation indicating $\nu > 0$. In addition, values of the dilatancy factor, $\beta$ of Rudnicki & Rice (1975) (see below), inferred by Olsson (1999) and Wong et al. (2001) correspond to increasing lateral deformation. The response in these experiments may, however, differ significantly from the isotropic response assume by the Rudnicki & Rice (1975) relation.

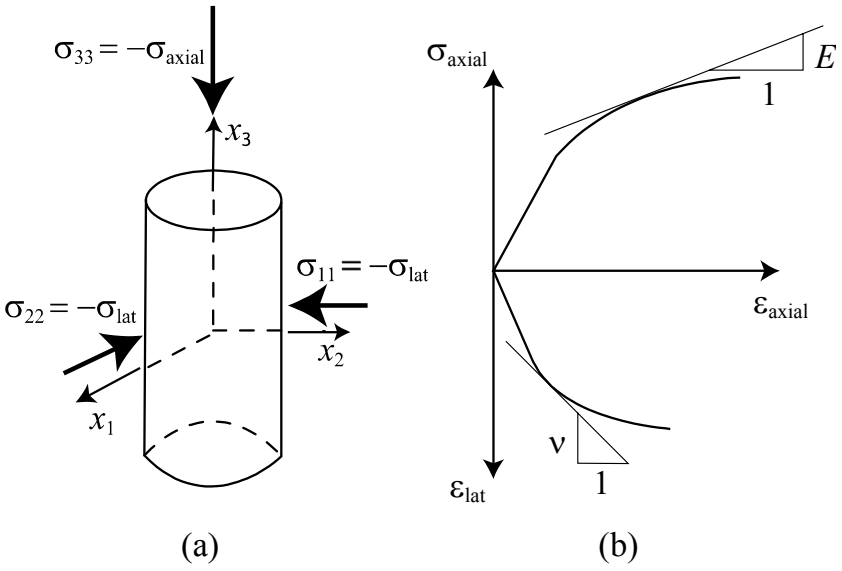


Figure 4. Schematic illustration of the axisymmetric compression test (a) and definitions of the constitutive parameters $E$ and $\nu$ for constant lateral stress used by Rudnicki (2002).

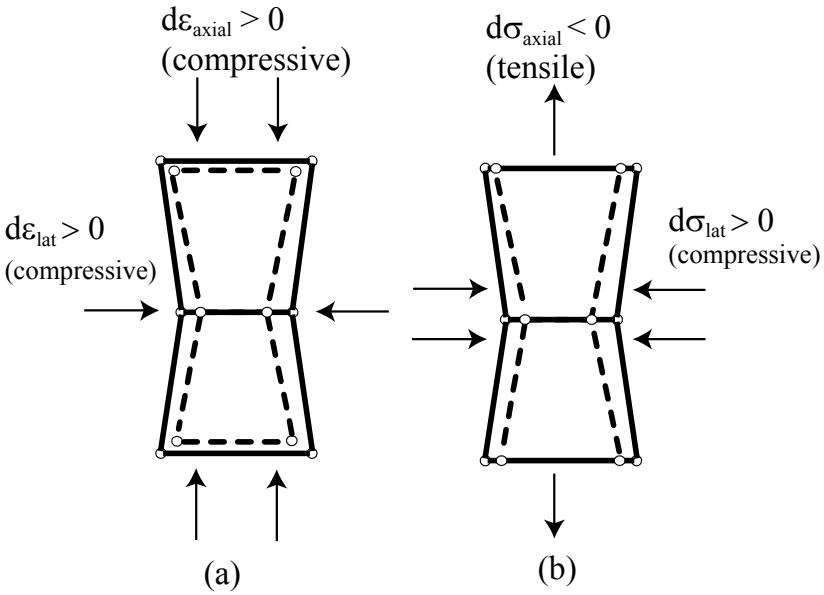

Figure 5. Mechanical model illustrating the possibility of $\mu < 0$ (a) and $r < 0$ (b).

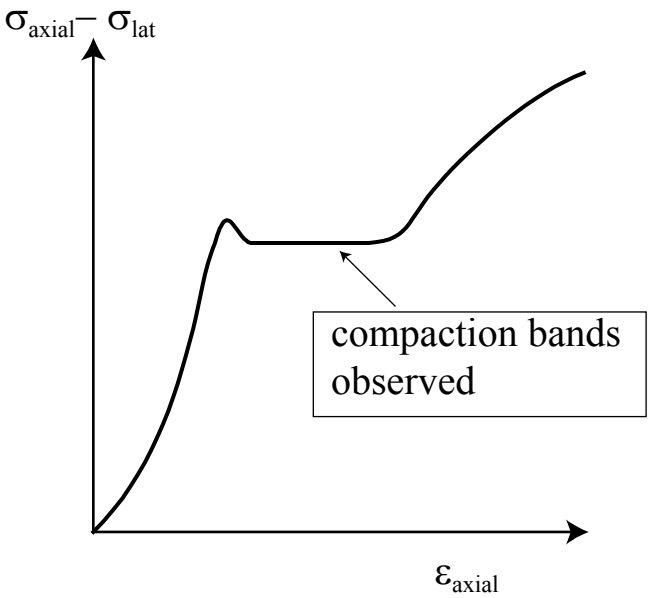

Figure 6. Schematic illustration of a typical axisymmetric compression stress – strain curve for a very porous sandstone.

### *4.2 General Deformation States*

Analyses of the inception of compaction bands for general deformation states have been based on modifications and extensions of the analysis of shear band inception by Rudnicki & Rice (1975). They noted the possibility of a bifurcation corresponding to localized deformation in a planar zone perpendicular to one of the principal stresses (such as a compaction band), but they did not elaborate because this case occurred for a range of constitutive parameters outside those for the low porosity rocks on which they were focusing. Ottosen & Runesson (1991) also identified the possibility of this type of bifurcation for a slightly more general constitutive model than

considered by Rudnicki & Rice (1975) and noted that it would occur for a material modeled with a yield surface "cap", which allows for yielding in hydrostatic compression (Dimaggio & Sandler, 1971). Ottosen & Runesson (1991) also found that the condition for the occurrence of this type of solution differed from that given by Rudnicki & Rice (1975). Perrin & Leblond (1993) corrected and discussed in detail this error in Rudnicki & Rice (1975).

Issen & Rudnicki (2000, 2001) give an extensive discussion of the possibilities for the occurrence of planar localized zones perpendicular to the most or least compressive principal stress and the interpretation of the former in terms of compaction zones. They do this within the constitutive framework used by Rudnicki & Rice (1975), the most general form for an incrementally linear elastic-plastic solid with yield surface and plastic potential depending on only the first and second stress invariants. Figure 7 shows such a yield surface described by

$$F(\tau, \sigma, H) = 0 \tag{10}$$

where $\tau = \sqrt{s_{ij} s_{ij} / 2}$ is the second invariant of the deviatoric stress, $s_{ij} = \sigma_{ij} - (1/3)\delta_{ij}\sigma_{kk}$, $\delta_{ij}$ is the Kronecker delta, $\sigma = -\sigma_{kk}/3$ is the mean normal stress (positive in compression) and $H$ denotes a set of one or more variables that describe the current state of plastic deformation. Figure 7 also shows the inelastic increments of the volume strain $d\varepsilon^p$ (positive in extension) and equivalent shear strain $d\gamma^p$ as components of a vector that is normal to the plastic potential surface. The friction coefficient used by Rudnicki & Rice (1975), $\mu$, is equal to the local slope of the yield surface $-(\partial F/\partial\sigma)/(\partial F/\partial\tau)$ and the dilatancy factor, $\beta$, is $d\varepsilon^p / d\gamma^p$. Because their primary interest was shear localization in low porosity, dilatant rocks, Rudnicki & Rice (1975) focused attention on the case $\beta$ and $\mu$ positive. But, as shown in Figure 7 and as noted by Issen & Rudnicki (2000), and previously by Ottosen & Runesson (1991) using different notation, $\beta$ and $\mu$ are negative on the "cap" portion of the yield surface.

The trajectory of the standard axisymmetric compression test in Figure 7 is a straight line with slope $\sqrt{3}$ that intersects the horizontal axis at the value of the constant lateral confining stress (Fig. 8). Consequently, tests at low confining stress will intersect the shear surface first and tests at higher confining stresses will intersect the cap first.

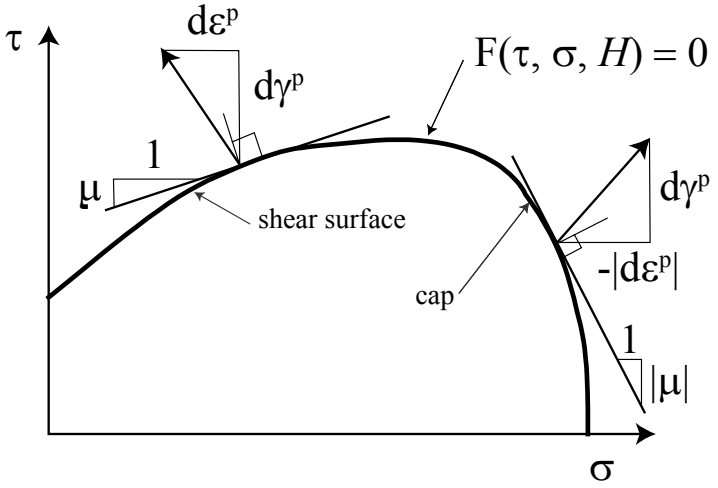


Figure 7. Illustration of a yield surface with a cap. The inelastic increment of strain is plotted as a vector. This vector is normal to the plastic potential surface, but not, in general, to the yield surface.

Issen & Rudnicki (2000), incorporating the correction of Perrin & Leblond (1993) find that compaction bands will precede shear bands if

$$\frac{1}{3}(\beta + \mu) \le \frac{(1-2\nu)N - \sqrt{4 - 3N^2}}{2(1+\nu)} \tag{11}$$

where $\nu$ is Poisson's ratio (equal to $\nu$ in (7) and (9) only for elastic deformation) and $N$ is a deviatoric stress state parameter equal to the intermediate principal deviatoric stress divided by $2\tau$. (An equivalent condition is given by Ottosen & Runesson (1991)). For axisymmetric compression $N = 1/\sqrt{3}$ and (11) reduces to

$$\beta + \mu \le -\sqrt{3} \tag{12}$$

Thus, compaction band formation is favored on the "cap" portion of the yield surface where $\beta$ and $\mu$ are negative. The corresponding critical value of the tangent modulus for constant lateral confining stress (obtained by combining (19) and (21) of Issen & Rudnicki (2000)) is

$$\frac{E}{2G(1+\nu)} = \frac{-(1+2\mu/\sqrt{3})(1+2\beta/\sqrt{3})}{(1-\nu)(1-\mu/\sqrt{3})(1-\beta/\sqrt{3}) - (1+2\mu/\sqrt{3})(1+2\beta/\sqrt{3})} \tag{13}$$

where $G$ is the elastic shear modulus and the combination in the denominator of the left hand side is Young's modulus.

The cap portion of the yield surface in Figure 7 connects smoothly to the shear surface. However, there is evidence (e.g. Wong et al. 1997, Wong & Baud, 1999) that the shear and cap portions are separate surfaces and they are often implemented as such in numerical calculations (e.g., Fossum et al. 1995, Fossum & Frederich, 2000). The simplest interpretation of the two surfaces is that they reflect different microscale mechanisms of inelasticity: shear-driven local tensile cracking and dilatancy for the shear surface and pore collapse and grain crushing for the cap. The evolutions of the cap and shear surfaces will be different, in general, and depend on different measures of inelastic deformation (e.g. accumulated inelastic volume strain or accumulated inelastic equivalent shear strain). Wong et al. (2001) have interpreted their data on Bentheim sandstone as requiring activation of multiple damage mechanisms. Figure 8 illustrates a yield surface in which the cap and shear portions intersect at a corner.

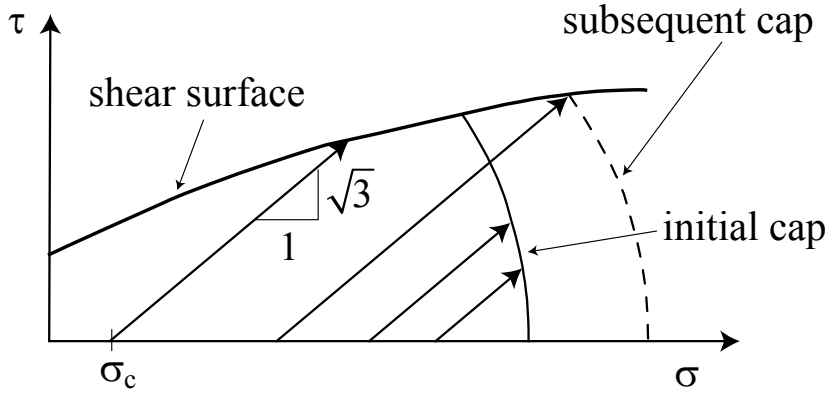


Figure 8. Illustration of a yield surface formed by separate shear and cap portions. Four trajectories of axisymmetric compression tests with different constant lateral confining pressure ($\sigma_c$) are also shown.

The additional flexibility of the direction of the inelastic strain increment vector at a yield surface corner is well known to enhance the possibility of localization (Rudnicki & Rice, 1975). Although it is unlikely that the stress path will intersect the corner on the initial yield surface, if the two surfaces evolve separately, increasing loads will cause the stress state to coincide with the corner (as illustrated by one trajectory in Fig. 8). The analysis of bifurcation conditions at a corner are much more complicated but some limiting results have been given by Issen (2002).

## 5 CONCLUDING DISCUSSION

Compaction bands have been observed in porous sandstones in the field and in laboratory axisymmetric compression tests on several varieties of sandstones. A bifurcation approach demonstrates that compaction bands are a possible alternative solution to homogeneous deformation for constitutive parameters that are appropriate for high porosity rock. In particular, inelastic volume compression and a shear yield stress that decreases with increasing mean compressive

stress favor formation of compaction bands. These features are characteristic of a "cap" yield surface often used to model the inelastic response of porous geomaterials.

There are, as yet, many open questions about the formation and evolution of compaction bands. Although the bands observed in the laboratory are similar to those observed in the field, their length scale is limited to the size of the laboratory specimen and, therefore, is much smaller. Furthermore, the bands observed in the laboratory tend to form first near the specimen ends and, consequently, appear to be triggered by slight nonuniformities caused by the end constraint. For these reasons, there remain questions about whether band formation in the field and laboratory are the same phenomenon.

Predictions for the inception of compaction band formation from bifurcation theory agree roughly with observations in the following sense: compaction band formation is predicted for constitutive parameters representative of porous sandstones. Numerical values of these parameters inferred from experiments are close to but do not agree in detail with those predicted by analysis. This discrepancy may be due to inadequacy of the constitutive model, inappropriateness of the bifurcation approach or uncertainties in the numerical determination of parameters. Predictions are sensitive to details of the structure and evolution (with nonelastic deformation) of the cap surface and the nature of its intersection with the shear surface. These features are not, at present, well-constrained by experiments.

Compaction band formation clearly requires high porosity (sandstones in which they have been observed range from about 15 to 30% porosity). There is, however, no theory explicitly connecting predictions to porosity, nor is it known from either experiments or theory whether there exists some critical minimum value of porosity. Because the porosity of natural materials cannot be controlled and is limited in range, this issue might be addressed profitably by experiments on man-made sintered materials. Although compaction band formation is roughly correlated with phenomenological nonelastic parameters, e.g. those of the cap model, little understanding exists of how band formation depends on the microstructure, e.g. grain size, shape, and distribution, cement and presence of clay minerals. Vardoulakis and Sulem (1995) do suggest, however, that compaction instabilities are more prevalent in geomaterials of uniform grain and pore sizes. Furthermore, DiGiovanni et al. (2000) have noted some differences in the micromechanical deformation mechanisms of Castlegate sandstone, in which compaction bands have been observed, from those of Berea sandstone (Menéndez et al. 1996)in which they have not.

The bifurcation analysis addresses the inception of band formation but not the subsequent evolution. Experiments have revealed that the evolution can have at least two quite different structures: widening of the compacted zone and widening of a pattern of compacted and uncompacted regions. Reasons for these different morphologies are not known.

The bifurcation analysis also suggests that there should be a transition from compaction bands to shear bands at high angles to the specimen axis for axisymmetric compression tests with decreasing values of the lateral confining pressure. Although both compaction bands and shear bands have been observed in some experiments, observations of very high angle shear bands are infrequent. More generally the nature of the transition between shear and compaction bands is unclear and likely depends on the nature of the intersection of the shear and cap surfaces.

The primary practical significance of compaction band formation and evolution is their role in altering the permeability structure of a formation. Experiments (Papamichos et al., 1993, Holcomb & Olsson, 2002) have demonstrated that compaction significantly reduces the permeability, but otherwise the effects of interaction of pore fluid have not been explored. In a different context, theoretical study of compaction of a fluid-saturated material with a nonlinear dependence of permeability on porosity suggests the possibility of solitary wave solutions (Barcilon & Richter, 1986). Predictive capability for field applications requires a better understanding of the role of pore pressure effects on evolution of the cap surface and of nonlinear effective stress effects on the permeability of compacting material.

*Acknowledgement.* I am grateful for numerous discussions with David Holcomb, Bill Olsson and Teng-fong Wong. I am also grateful to Lallit Anand for bringing to my attention the connection with non-uniform compaction of sintered materials. Partial financial support for this research has been provided by the U. S. Department of Energy, Office of Basic Energy Sciences under Grant DE-FG-02-93ER14344 to Northwestern University.

REFERENCES


Antonellini, M. & Aydin, A. 1995. Effect of faulting on fluid flow in porous sandstones: geometry and spatial distribution. *Am. Assoc. Petrol. Geol*. 79: 642-671.

Barcilon, V. & Richter, F. M. 1986. Nonlinear waves in compacting media. *J. Fluid Mech*. 164: 429-448.

Bastawros, A-F., Bart-Smith, H. & Evans, A. G. 2000. Experimental analysis of deformation mechanisms in a closed-cell aluminum alloy foam. *J. Mech. Phys. Solids* 48:301-322.

Bésuelle, P. 2001. Compacting and dilating shear bands in porous rock: theoretical and experimental conditions. *J. Geophys. Res*. 106: 13435-13442.

Chambon, R. 1986. Bifurcation par localization en bande de disaillement, une approache aved des lois incrémentalement non linéaires. *J. Méc. Théor. Appl*. 5(2): 277-298.

DiGiovanni, A. A., Fredrich, J. T., Holcomb, D. J. & Olsson, W. A. 2000. Micromechanics of compaction in an analogue reservoir sandstone. In J. Girard, M. Liebman, C. Breeds, & T. Doe (eds.), *Pacific Rocks* 2000: 1153-1158. Rotterdam: Balkema.

Dimaggio, F. L. & Sandler, I. S. 1971. Material model for granular soils. *J. Engn. Mech., ASCE* 97: 935-950.

Fossum, A. F., Senseny, P. E., Pfeifle, T. W. & Mellegard, K. D. 1995. Experimental determination of probability distributions for parameters of a salem limestone cap plasticity model. *Mech. Mat*. 21:119-137.

Fossum, A. F. & Fredrich, J. T. 2000. Cap plasticity models and compactive and dilatant pre-failure deformations. In J. Girard, M. Liebman, C. Breeds, & T. Doe (eds.), *Pacific Rocks* 2000: 1169-1176. Rotterdam: Balkema.

Gu, C., Kim, M. & Anand, L. 2001. Constitutive equations for metal powders: application to powder forming processes. *Int. J. Plasticity* 17: 147-209.

Haimson, B. C. 2001. Fracture-like borehole breakouts in high-porosity sandstone: are they caused by compaction bands? *Phys. Chem. Earth (A)* 26: 15-20.

Holcomb, D. J. & Olsson, W. A. 2002. Compaction localization and fluid flow. Submitted to *J. Geophys. Res*.

Issen, K. A. & Rudnicki, J. W. 2000. Conditions for compaction bands in porous rock. *J. Geophys. Res*. 105: 21529-21536.

Issen, K. A. & Rudnicki, J. W. 2001. Theory of compaction bands in porous rock. *Phys. Chem. Earth (A)* 26:95-100.

Issen, K. A.. 2002. The influence of constitutive models on localization conditions for porous rock, *Engn. Frac. Mech.* 69: 1891-1906.

Klein, E., Baud, P., Reuschle, T., & Wong, T-f. 2001. Mechanical behaviour and failure mode of Bentheim sandstone under triaxial compression. *Phys. Chem. Earth (A)* 26: 21-25.

Menéndez, B., Zhu, W., & Wong T.-f. 1996. Micromechanics of brittle faulting and cataclastic flw in Berea sandstone. *J. Struct. Geol*. 18(1): 1-16.

Mollema, P. N. & Antonellini, M. A. 1996. Compaction bands: a structural analog for anti-mode I cracks in aeolian sandstone. *Tectonophysics* 267: 209-228.

Nagel, N. B. 2001. Compaction and subsidence issues within the petroleum industry: from Wilmington to Ekofisk and beyond. *Phys. Chem. Earth (A)* 26: 3-14.

Olsson, W. A. 1999. Theoretical and experimental investigation of compaction bands in porous rock, *J. Geophys. Res*. 104: 7219-7228.

Olsson, W. A. 2001. Quasistatic propagation of compaction fronts in porous rock. *Mech. Mat.* 33: 659-668.

Olsson, W. A. & Holcomb, D. J. 2000. Compaction localization in porous rock. *Geophys. Res. Letters*, 27: 3537-3540.

Olsson, W. A., Holcomb, D. J. & Rudnicki, J. W. 2002. Compaction localization in porous sandstone: implications for reservoir compaction. *Oil & Gas Science and Technology, Revue de l'institut Français du Pétrole* 57 (5): 591-599.

Ottosen, N. S. & K. Runesson, K. 1991. Properties of discontinuous bifurcation solutions in elasto-plasticity. *Int. J. Solids Struct*. 27 (4): 401-421.

Papamichos, E., Vardoulakis, I. & Quadfel, H. 1993. Permeability reduction due to grain crushing around a perforation. *Int. J. Rock Mech. Min. Sci. Geomech. Abstr*. 30:1223-1229.

Papka, S. D. & Kyriakides, S. 1998. In-plane crushing of a polycarbonate honeycomb. *Int. J. Solids Struct*. 35: 239-267.

Park, C. & Nutt, S. R. 2001. Anisotropy and strain localization in steel foam. *Mat. Sci. Eng*. A299: 68-74.

Perrin, G. & LeBlond, J. B. 1993. Rudnicki and Rice's analysis of strain localization revisited. *J. Appl. Mech.* 60**:** 842-846.

Rice, J. R. 1976. The localization of plastic deformation. In W. Koiter (ed.), *Theoretical and Applied Mechanics, Proc. 14th IUTAM Congress*: 207-220. Amsterdam: North Holland.

Rice, J. R. & Rudnicki, J. W. 1980. A note on some features of the theory of localization of deformation. *Int. J. Solids Struct.* 16: 597-605.

Rudnicki, J. W. 1977. The effect of stress-induced anisotropy on a model of brittle rock failure as localization of deformation. In F.-D. Wang & G. B. Clark (eds.), *Energy Resources and Excavation Technology, Proceedings of the 18th U. S. Symposium on Rock Mechanics*: 3B4- - 3B4-8.

Rudnicki, J. W. 2002. Conditions for compaction and shear bands in a transversely isotropic material. *Int. J. Solids Struct.* 39 (13-14): 3741-3756.

Rudnicki, J. W. & Rice, J. R. 1975. Conditions for the localization of deformation in pressure-sensitive dilatant materials. *J. Mech. Phys. Solids* 23: 371-394.

Vardoulakis, I. & Sulem, J. 1995. *Bifurcation Analysis in Geomechanics*. Glasgow: Blackie Academic.

Wawersik, W. R., Rudnicki, J. W., Dove, P., Harris, J., Logan, J. M., Pyrak-Nolte, L., Orr, F. M., Jr., Ortoleva, P. J., Richter, F., Warpinski, N., Wilson, J. L. & Wong, T.-f. 2001. Terrestrial sequestration of CO2: An assessment of research needs. In *Advances in Geophysics* 43: 97-177.

Wong, T-f., Baud, P. & Klein, E. 2001. Localized failure modes in a compactant porous rock, *Geophys. Res. Lett*. 28: 2521-2524.